



Cite this: *Chem. Commun.*, 2014, 50, 15191

Received 25th August 2014,
Accepted 8th October 2014

DOI: 10.1039/c4cc06693f

www.rsc.org/chemcomm

Magnetic blocking in extended metal atom chains: a pentachromium(II) complex behaving as a single-molecule magnet†

A. Cornia,^{*a} L. Rigamonti,^a S. Boccedi,^a R. Clérac,^{bc} M. Rouzières^{bc} and L. Sorace^d

Compound $[\text{Cr}_5(\text{tpda})_4\text{Cl}_2]$ ($\text{H}_2\text{tpda} = \text{N}^2, \text{N}^6$ -di(pyridin-2-yl)pyridine-2,6-diamine), an Extended Metal Atom Chain complex featuring two quadruply-bonded $\{\text{Cr}_2\}$ units, exhibits field-induced slow relaxation of its magnetization arising from the terminal chromium(II) ion and provides the first example of a chromium(II)-based Single-Molecule Magnet.

Individual molecules with a directionally-bistable magnetic moment, called Single-Molecule Magnets (SMMs),¹ are considered the smallest, chemically-tuneable components for spin-based devices.²

In the simplest case, a SMM possesses a ground state with a large total spin (S_T) and an easy-axis (z) magnetic anisotropy, which partially lifts the $2S_T + 1$ -fold degeneracy of the ground state in zero magnetic field. Such zero-field splitting (zfs) is described by the Hamiltonian $\hat{\mathcal{H}}_{\text{zfs}} = D\hat{S}_{T,z}^2 + \hat{\mathcal{H}}'$, where the first term (with $D < 0$) is dominant and causes the $M_S = \pm S_T$ states to lie lowest in energy. If magnetization relaxation occurs by a multistep Orbach process, magnetic blocking is observed at temperatures such that $k_B T \ll U$, where U is the total energy splitting of the multiplet. However, nondiagonal terms in the Hamiltonian ($\hat{\mathcal{H}}'$), like rhombic or higher-order transverse anisotropies, can mix wavefunctions with the same $|M_S|$, thereby opening new pathways for relaxation *via* quantum tunnelling.¹ Their effect increases with decreasing S_T , thus explaining why slow relaxation of the magnetization is comparatively less frequent in mononuclear than in polynuclear complexes, where higher S_T can be reached.

SMM behaviour was indeed found in a variety of mononuclear species containing $3d$,^{3–5} $5d$,⁶ $4f^{7a,b}$ or $5f^{7c}$ ions, but the relaxation mechanisms often deviate from the above-described scheme. First, most of these systems feature an unquenched orbital angular momentum and consequently do not exhibit spin-only‡ magnetism.^{3,7} More unexpectedly, magnetic blocking can arise in individual Kramers ions (*e.g.* Co^{2+} , Dy^{3+}) with a predominantly easy-plane magnetic anisotropy.⁸ Here, magnetization relaxation occurs *via* non-Orbach mechanisms that produce a distinct curvature in an Arrhenius plot. Unlike tunnelling effects, they result in non-physical values of the activation barrier when a linear fit is attempted over high-temperature data.^{8a} Examples of spin-only‡ mononuclear species relaxing *via* a genuine overbarrier process are found in Jahn–Teller distorted Mn^{3+} complexes.⁵

Although isoelectronic with Mn^{3+} , Cr^{2+} has been rarely used in molecular magnetism primarily because of its propensity toward oxidation.⁹ We herein report the SMM properties of a Cr^{2+} -based complex belonging to the popular class of Extended Metal Atom Chains (EMACs). EMACs have been extensively studied in the past as molecular wires and as benchmark systems for understanding metal–metal interactions.¹⁰ In an EMAC, an array of metal ions is kept aligned in a string by four oligopyridylamide (or related) ligands. The compound $[\text{Cr}_5(\text{tpda})_4\text{Cl}_2]$ (**1**, $\text{H}_2\text{tpda} = \text{N}^2, \text{N}^6$ -di(pyridin-2-yl)pyridine-2,6-diamine) was the focus of a particularly lively debate regarding bond delocalization.^{11,12} From X-ray structural and magnetic data it was finally shown that **1** and related pentachromium(II) strings are *unsymmetrical* in the solid state and contain two diamagnetic pairs of quadruply-bonded metals *plus* one terminal high-spin Cr^{2+} ion^{13,14} (Fig. 1).

Such a bonding scheme is evident from the $\text{Cr} \cdots \text{Cr}$ distances found in $1 \cdot 4\text{CHCl}_3 \cdot 2\text{Et}_2\text{O}$: (from Cr1 to Cr5) 2.598(3), 1.872(2), 2.609(2) and 1.963(3) Å.^{12b} As a consequence, these compounds and the related tri-,^{15a–c} hepta-^{15d} and nonachromium(II)^{15e} species have an $S_T = 2$ ground state. On account of the negative D parameter and small rhombicity reported for $[\text{Cr}_3(\text{dpa})_4\text{Cl}_2] \cdot \text{CH}_2\text{Cl}_2$ ($2 \cdot \text{CH}_2\text{Cl}_2$, $\text{Hdpa} = \text{dipyridin-2-ylamine}$),^{15c} we have carried out a complete magnetic susceptibility study on $1 \cdot 4\text{CHCl}_3 \cdot 2\text{Et}_2\text{O}$. Our data show field-induced slow relaxation of the magnetization

^a Dipartimento di Scienze Chimiche e Geologiche, Università degli Studi di Modena e Reggio Emilia & INSTM RU of Modena and Reggio Emilia, via G. Campi 183, 41125 Modena, Italy. E-mail: acornia@unimore.it

^b CNRS, CRPP, UPR 8641, F-33600 Pessac, France

^c Univ. Bordeaux, CRPP, UPR 8641, F-33600 Pessac, France

^d Laboratory of Molecular Magnetism (LaMM), Dipartimento di Chimica 'Ugo Schiff', Università degli Studi di Firenze & INSTM RU of Firenze, via della Lastruccia 3-13, 50019 Sesto Fiorentino (FI), Italy

† Electronic supplementary information (ESI) available: Synthetic details, additional magnetic characterization data, details of Angular Overlap Model calculations. See DOI: 10.1039/c4cc06693f



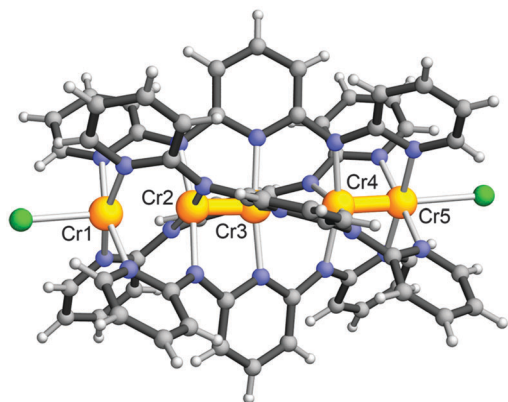


Fig. 1 Molecular structure of **1** in $1.4\text{CHCl}_3 \cdot 2\text{Et}_2\text{O}$, as reported by Cotton *et al.*^{12b} Colour code: orange = Cr, green = Cl, grey = C, blue = N, light grey = H. Diamagnetic pairs of chromium(II) ions are highlighted using thick bonds.

compatible with an Orbach mechanism, thereby bridging both EMAC and SMM research fields.

$1.4\text{CHCl}_3 \cdot 2\text{Et}_2\text{O}$ was synthesised as originally reported by Peng's group¹¹ and isolated as large, deep-brown crystals by vapour diffusion of diethyl ether into a chloroform solution of the complex. The compound was checked by Matrix-Assisted Laser Desorption/Ionization Time-of-Flight and Electrospray Ionization mass spectrometries as well as by single-crystal X-ray diffraction, elemental analysis and IR spectroscopy (see ESI†). Unless kept in contact with the mother solution, crystals of $1.4\text{CHCl}_3 \cdot 2\text{Et}_2\text{O}$ progressively lose lattice solvent molecules. To avoid large uncertainties in molecular mass, the sample used for magnetic characterization was subject to prolonged vacuum pumping in order to remove all volatiles. However, wet crystals displayed the same static and dynamic magnetic properties as this vacuum-treated sample (see ESI†). The χT product measured at 1 kOe (Fig. 2) amounts to $2.89 \text{ cm}^3 \text{ K mol}^{-1}$ at 300–320 K and is virtually temperature independent down to 100 K, but decreases significantly at a

lower temperature reaching $2.21 \text{ cm}^3 \text{ K mol}^{-1}$ at 1.85 K. The room temperature value is close to the expectation for an $S_T = 2$ spin with $g = 1.963$, in agreement with $g < 2.00$ for high-spin chromium(II).¹⁶

To better probe the ground state properties, the isothermal magnetization was measured up to 70 kOe at temperatures ranging from 1.9 to 10 K (Fig. 2). Although the magnetization does not reach saturation in the H and T range explored, its highest measured value ($3.77 N_A \mu_B$) is close to the saturation magnetization for an $S_T = 2$ state with $g = 2$ (*i.e.* $4 N_A \mu_B$). When plotted as a function of H/T (see ESI†), the curves display a pronounced nesting which hints to deviations from the Brillouin function. Such a behaviour was modelled by introducing magnetic anisotropy effects, through spin Hamiltonian $\hat{\mathcal{H}}_{\text{ZFS}}$ and assuming an isotropic g factor. Setting $S_T = 2$ and $\hat{\mathcal{H}}' = 0$, M versus H data could be accurately fitted with $D = -1.510(6) \text{ cm}^{-1}$ ($D/k_B = -2.173(9) \text{ K}$) and $g = 1.9731(8)$. Imposing a positive D parameter resulted in a much worse fit. W-band ($\nu \approx 94 \text{ GHz}$) EPR spectroscopy (Fig. 3) confirmed the spin value and the easy-axis anisotropy, with only very weak rhombicity. Best simulations¹⁷ were obtained using spin Hamiltonian $\hat{\mathcal{H}}_{\text{EPR}} = \mu_B \hat{S}_T \cdot \mathbf{g} \cdot \hat{\mathbf{H}} + D \hat{S}_{T,z}^2 + E(\hat{S}_{T,x}^2 - \hat{S}_{T,y}^2)$ with parameters: $g_x = g_y = 1.990(3)$, $g_z = 1.975(2)$, $D = -1.53(1) \text{ cm}^{-1}$ ($D/k_B = -2.20(1) \text{ K}$) and $|E/D| = 6(2) \times 10^{-3}$. It is to be stressed that, even if $|D| \approx h\nu$ and the simplification induced by the high field limit is not yet reached, the temperature dependence of the spectrum is only compatible with a negative D value (see ESI†). The very small rhombicity and the easy-axis anisotropy are consistent with the environment of the terminal chromium(II) ion, which features a square-pyramidal coordination sphere (CrN_4Cl) with the four basal nitrogen donors at $2.13(1) \text{ \AA}$, the apical chloride ion at 2.46 \AA and the N–Cr–N angles in the range $87.5\text{--}90.9^\circ$ (Fig. 1). Significantly, the anisotropy parameters are comparable with those found in $2\text{-CH}_2\text{Cl}_2$ by high-frequency EPR ($D = -1.643(1) \text{ cm}^{-1}$ or $D/k_B = -2.364(1) \text{ K}$, $E = 0.0339(4) \text{ cm}^{-1}$ or $E/k_B = 0.0488(6) \text{ K}$)^{15c} and are consistently reproduced by Angular Overlap Model calculations (see ESI†).

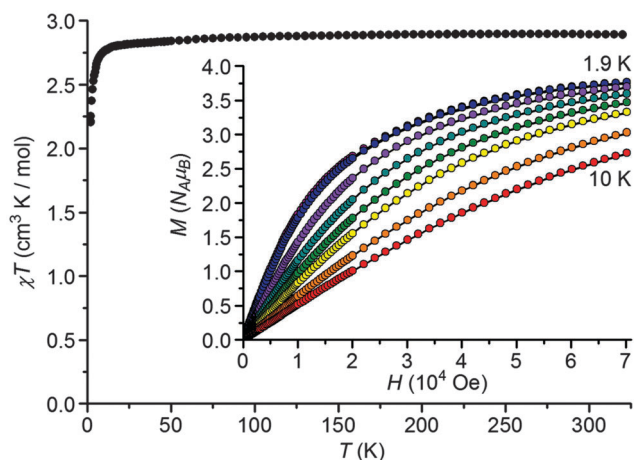


Fig. 2 χT versus T plot for **1** at 1 kOe. The inset presents M versus H data measured at eight different temperatures (1.9, 2.0, 3.0, 4.0, 5.0, 6.0, 8.0 and 10.0 K), along with the best-fit curves with the parameters reported in the text.

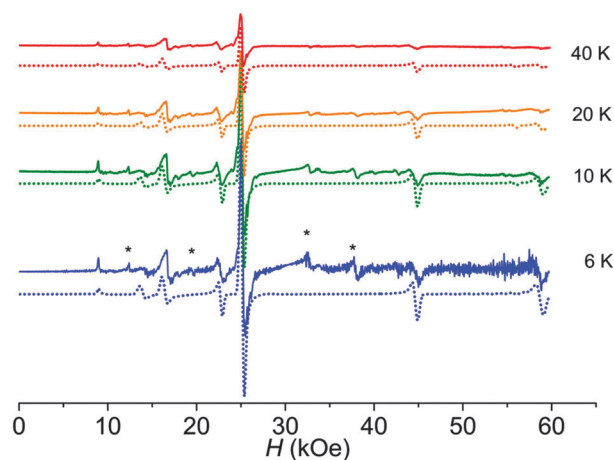


Fig. 3 Experimental (continuous lines) and best simulation (dotted lines) W-band EPR spectra of **1**. The asterisks mark spurious signals arising from incomplete powder averaging due to the preparation of the sample (see ESI†).



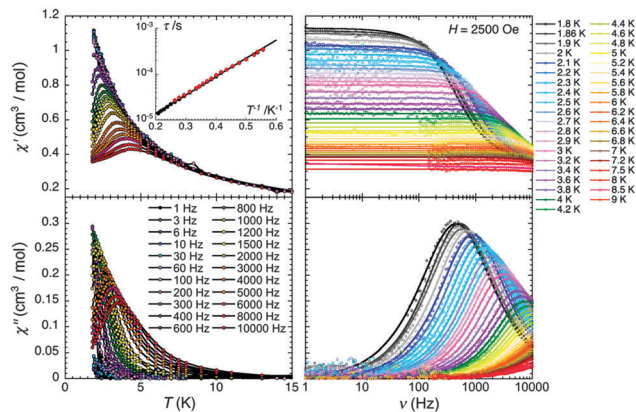


Fig. 4 Temperature (left) and frequency (right) dependence of the real (χ' , top) and imaginary (χ'' , bottom) parts of the ac susceptibility, between 1 and 10 000 Hz and between 1.8 and 9 K, respectively, for **1** in 2500 Oe dc field. While solid lines on the left-hand figures are visual guides, the solid curves on the right-hand figures provide the best fit using the generalized Debye model.¹⁸ Inset: τ versus T^{-1} plot for **1** in 2500 Oe dc field. The relaxation time (τ) has been estimated from the generalized Debye fit of the χ' versus ν (red dots) and χ'' versus ν (black dots) data between 1.8 and 4.8 K. Solid line is the best fit to the Arrhenius law.

In spite of the small spin value ($S_T = 2$), the significant easy-axis anisotropy of **1** induces in-field slow relaxation of the magnetization at low temperature. The alternating current (ac) magnetic susceptibility of **1** was investigated in the 1.8–15 K temperature range and with frequencies up to 10 000 Hz (see ESI†). In zero static field, simple paramagnetic behaviour was observed in the probed range of frequency and temperature. Application of a static field was however effective in slowing down the relaxation leading to the appearance of an out-of-phase signal. The optimal field of 2.5 kOe was located in a preliminary scan from 0 to 10 kOe at 1.8 K and was used for temperature dependent studies. The analysis of the resulting $\chi'(\nu)$ and $\chi''(\nu)$ curves from 1.8 to 4.8 K was based on the generalized Debye model¹⁸ and provided the temperature dependence of the relaxation time τ . A semi-logarithmic plot of τ versus T^{-1} evidences a thermally-activated relaxation mechanism with an effective barrier $U_{\text{eff}}/k_B = 9.2(5)$ K (Fig. 4) and an attempt time $\tau_0 = 2.2(5) \times 10^{-6}$ s. Within experimental error, U_{eff} equals the total splitting of the $S_T = 2$ multiplet ($U/k_B = (|D|/k_B)S_T^2 = 8.81(6)$ K). This suggests that in-field relaxation follows an overbarrier Orbach mechanism¹ and that $\pm M_S$ states are not heavily admixed, in spite of the small and integer S_T value. The residual mixing is however enough to produce fast relaxation in zero field. To the best of our knowledge, this represents the first example of a chromium(II)-based SMM. In this respect, the string-like structure of **1** and the arrangement of the tpda^{2-} ligands enforce the metal ions in an almost perfectly axial environment which is suitable for SMM behaviour.

In our ongoing efforts we are now looking for more examples of Cr^{2+} -based SMM-EMACs through variation of the axial ligands and of the chain length. In addition, we are exploring the magnetization dynamics of EMACs containing heavier and more anisotropic transition-metal ions, like Ru^{2+} .¹⁹

We thank Italian MIUR for funding through a FIRB project (RBAP117RWN). Financial support from University of Bordeaux, the ANR, the Région Aquitaine, CNRS and Ente CRF is also gratefully acknowledged. We are indebted to Prof. R. Sessoli and Dr G. Poneti (Università degli Studi di Firenze) for carrying out preliminary magnetic measurements.

Notes and references

‡ The term “spin only” is used here for metal centers with no first-order orbital angular momentum; in such systems, orbital contributions to magnetic behaviour can nevertheless arise *via* second-order spin-orbit coupling.

- 1 D. Gatteschi, R. Sessoli and J. Villain, *Molecular Nanomagnets*, Oxford University Press, Oxford, UK, 2006.
- 2 (a) F. Zu, Z. Liu, K. Yao, G. Gao, H. Fu, S. Zhu, Y. Ni and L. Peng, *Sci. Rep.*, 2014, **4**, 4838; (b) S. Thiele, F. Balestro, R. Ballou, S. Klyatskaya, M. Ruben and W. Wernsdorfer, *Science*, 2014, **344**, 1135–1138.
- 3 (a) J. M. Zadrozny, D. J. Xiao, M. Atanasov, G. J. Long, F. Grandjean, F. Neese and J. R. Long, *Nat. Chem.*, 2013, **5**, 577–581; (b) J. M. Zadrozny, M. Atanasov, A. M. Bryan, C.-Y. Lin, B. D. Reinken, P. P. Power, F. Neese and J. R. Long, *Chem. Sci.*, 2013, **4**, 125–138; (c) M. Atanasov, J. M. Zadrozny, J. R. Long and F. Neese, *Chem. Sci.*, 2013, **4**, 139–156.
- 4 (a) J. M. Zadrozny and J. R. Long, *J. Am. Chem. Soc.*, 2011, **133**, 20732–20734; (b) J. Vallejo, I. Castro, R. Ruiz-García, J. Cano, M. Julve, F. Lloret, G. De Munno, W. Wernsdorfer and E. Pardo, *J. Am. Chem. Soc.*, 2012, **134**, 15704–15707; (c) J. M. Zadrozny, J. Liu, N. A. Piro, C. J. Chang, S. Hill and J. R. Long, *Chem. Commun.*, 2012, **48**, 3927–3929.
- 5 J. Vallejo, A. Pascual-Álvarez, J. Cano, I. Castro, M. Julve, F. Lloret, J. Krzystek, G. De Munno, D. Armentano, W. Wernsdorfer, R. Ruiz-García and E. Pardo, *Angew. Chem., Int. Ed.*, 2013, **52**, 14075–14079.
- 6 (a) K. S. Pedersen, M. Signist, M. A. Sørensen, A.-L. Barra, T. Weyhermüller, S. Piligkos, C. Aa. Thuesen, M. G. Vinum, H. Mutka, H. Weihe, R. Clérac and J. Bendix, *Angew. Chem., Int. Ed.*, 2014, **53**, 1351–1354; (b) J. Martínez-Lillo, T. F. Mastropietro, E. Lhotel, C. Paulsen, J. Cano, G. De Munno, J. Faus, F. Lloret, M. Julve, S. Nellutla and J. Krzystek, *J. Am. Chem. Soc.*, 2013, **135**, 13737–13748.
- 7 (a) H. L. C. Feltham and S. Brooker, *Coord. Chem. Rev.*, 2014, **276**, 1–33; (b) D. N. Woodruff, R. E. P. Winpenny and R. A. Layfield, *Chem. Rev.*, 2013, **113**, 5110–5148; (c) J. J. Baldoví, S. Cardona-Serra, J. M. Clemente-Juan, E. Coronado and A. Gaita-Ariño, *Chem. Sci.*, 2013, **4**, 938–946.
- 8 (a) E. Lucaccini, L. Sorace, M. Perfetti, J.-P. Costes and R. Sessoli, *Chem. Commun.*, 2014, **50**, 1648–1651; (b) S. Gómez-Coca, A. Urtizberea, E. Cremades, P. J. Alonso, A. Camón, E. Ruiz and F. Luis, *Nat. Commun.*, 2014, **5**, 4300.
- 9 (a) P. A. Lay and A. Levina, in *Comprehensive Coordination Chemistry II*, ed. J. A. McCleverty and T. J. Meyer, Elsevier, Amsterdam, The Netherlands, 2004, vol. 4, pp. 313–413; (b) T. Mallah, S. Thiébaud, M. Verdagner and P. Veillet, *Science*, 1993, **262**, 1554–1557; (c) C. Bellitto, F. Federici and S. A. Ibrahim, *Chem. Mater.*, 1998, **10**, 1076–1082.
- 10 (a) V. P. Georgiev, P. J. Mohan, D. DeBrincat and J. E. McGrady, *Coord. Chem. Rev.*, 2013, **257**, 290–298; (b) *Multiple Bonds Between Metal Atoms*, ed. F. A. Cotton, C. A. Murillo and R. A. Watson, Springer, New York, USA, 2006; (c) J. F. Berry, *Struct. Bond.*, 2010, **136**, 1–28.
- 11 H.-C. Chang, J.-T. Li, C.-C. Wang, T.-W. Lin, H.-C. Lee, G.-H. Lee and S.-M. Peng, *Eur. J. Inorg. Chem.*, 1999, 1243–1251.
- 12 (a) F. A. Cotton, L. M. Daniels, T. Lu, C. A. Murillo and X. Wang, *J. Chem. Soc., Dalton Trans.*, 1999, 517–518; (b) F. A. Cotton, L. M. Daniels, C. A. Murillo and X. Wang, *Chem. Commun.*, 1999, 2461–2462.
- 13 J. F. Berry, F. A. Cotton, C. S. Fewox, T. Lu, C. A. Murillo and X. Wang, *Dalton Trans.*, 2004, 2297–2302.
- 14 W.-Z. Wang, R. H. Ismayilov, G.-H. Lee, Y.-L. Huang, C.-Y. Yeh, M.-D. Fu, C.-H. Chen and S.-M. Peng, *New J. Chem.*, 2012, **36**, 632–637.
- 15 (a) R. Clérac, F. A. Cotton, L. M. Daniels, K. R. Dunbar, C. A. Murillo and I. Pascual, *Inorg. Chem.*, 2000, **39**, 748–751; (b) J. F. Berry, F. A. Cotton, T. Lu, C. A. Murillo, B. K. Roberts and X. Wang, *J. Am. Chem. Soc.*, 2004, **126**, 7082–7096; (c) J. Wang, Z. Wang, R. J. Clark,



- A. Ozarowski, J. van Tol and N. S. Dalal, *Polyhedron*, 2011, **30**, 3058–3061; (d) R. H. Ismayilov, W.-Z. Wang, G.-H. Lee, C.-H. Chien, C.-H. Jiang, C.-L. Chiu, C.-Y. Yeh and S.-M. Peng, *Eur. J. Inorg. Chem.*, 2009, 2110–2120; (e) R. H. Ismayilov, W.-Z. Wang, R.-R. Wang, C.-Y. Yeh, G.-H. Lee and S.-M. Peng, *Chem. Commun.*, 2007, 1121–1123.
- 16 (a) A.-L. Barra, A. Døssing, T. Morsing and J. Vibenholt, *Inorg. Chim. Acta*, 2011, **373**, 266–269; (b) J. Telsler, L. A. Pardi, J. Krzystek and L.-C. Brunel, *Inorg. Chem.*, 1998, **37**, 5769–5775.
- 17 S. Stoll and A. Schweiger, *J. Magn. Reson.*, 2006, **178**, 42–55.
- 18 (a) K. S. Cole and R. H. Cole, *J. Chem. Phys.*, 1941, **9**, 341–352; (b) C. Dekker, A. F. M. Arts, H. W. de Wijn, A. J. van Duyneveldt and J. A. Mydosh, *Phys. Rev. B: Condens. Matter Mater. Phys.*, 1989, **40**, 11243–11251.
- 19 C. Yin, G.-C. Huang, C.-K. Kuo, M.-D. Fu, H.-C. Lu, J.-H. Ke, K.-N. Shih, Y.-L. Huang, G.-H. Lee, C.-Y. Yeh, C.-H. Chen and S.-M. Peng, *J. Am. Chem. Soc.*, 2008, **130**, 10090–10092.

